

Quantum Curriculum Learning

Quoc Hoan Tran,^{*} Yasuhiro Endo, and Hirotaka Oshima

Quantum Laboratory, Fujitsu Research, Fujitsu Limited, Kawasaki, Kanagawa 211-8588, Japan

(Dated: July 12, 2024)

Quantum machine learning (QML) requires significant quantum resources to achieve quantum advantage. Research should prioritize both the efficient design of quantum architectures and the development of learning strategies to optimize resource usage. We propose a framework called quantum curriculum learning (Q-CurL) for quantum data, where the curriculum introduces simpler tasks or data to the learning model before progressing to more challenging ones. We define the curriculum criteria based on the data density ratio between tasks to determine the curriculum order. We also implement a dynamic learning schedule to emphasize the significance of quantum data in optimizing the loss function. Empirical evidence shows that Q-CurL significantly enhances the training convergence and the generalization for unitary learning tasks and improves the robustness of quantum phase recognition tasks. Our framework provides a general learning strategy, bringing QML closer to realizing practical advantages.

Introduction.— In the emerging field of quantum computing (QC), there is promise in using quantum computers at sufficiently large scales to solve certain machine learning (ML) problems much more efficiently than classical methods. This synergy between ML and QC has led to the creation of a new field known as quantum machine learning (QML) [1, 2], even though the practicality of its applications remains unclear. There is a question as to whether speed is the only metric by which QML algorithms should be judged [3]. In fact, classical ML focuses on identifying and reproducing features from data statistics. The initial hope is that QML can detect correlations in the classical data or generate new patterns that would be difficult for classical algorithms to achieve [4–8]. However, there is no clear evidence that analyzing classical data inherently requires quantum effects. This suggests a fundamental shift in the research community’s perspective: it is preferable to use QML on data that is already quantum in nature [9–14].

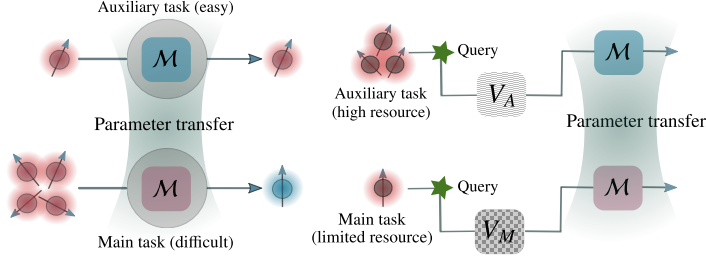
The typical learning process in QML involves extensive exploration within the domain landscape of a loss function. This function measures the discrepancy between the quantum model’s predictions and the actual values, aiming to locate its minimum using classical computers. However, the optimization often encounters pitfalls such as getting trapped in local minima [15, 16] or barren plateau regions [17]. These scenarios require substantial quantum computational resources to navigate the loss landscape successfully. Additionally, improving task accuracies necessitates evaluating numerous model configurations, especially against extensive datasets. Given the limitation of current quantum resources, this poses a considerable challenge. Therefore, in designing QML models, we must focus not only on their architectural aspects but also on efficient learning strategies.

The perspective of quantum resources refocuses our attention on the concept of learning. In ML, learning refers to the process through which a computer system enhances its performance on a specific task over time

by acquiring and integrating knowledge or patterns from data. We can improve current QML algorithms by making this process more efficient. For example, curriculum learning [18] is inspired by the human learning process, based on the intuitive observation that we often begin with simpler concepts before progressing to more complex ones. This insight leads to the development of a strategy for sampling or task scheduling—a curriculum—that introduces simpler samples or tasks to the model before moving on to more challenging ones. Although curriculum learning has been extensively applied and studied in classical ML [19–21], its exploration in the QML field, especially regarding quantum data, is still in the early stages. The most relevant research has focused on investigating model transfer learning within hybrid classical-quantum neural networks [22]. Typically, this involves starting with a pre-trained classical network that is then modified and enhanced by adding a variational quantum circuit at its final layer. Despite the potential benefits, there is still a lack of concrete evidence that effectively using a curriculum learning framework to schedule tasks and samples improves QML techniques.

In this Letter, we explore the potential of curriculum learning within the context of QML using quantum data. We demonstrate the feasibility of implementing curriculum learning in a quantum framework called quantum curriculum learning (Q-CurL). We consider two common scenarios in training QML models. First, a main task, which may be challenging or limited by data availability, can be facilitated through the preparatory parameter adjustment of an auxiliary task. This auxiliary task is comparatively easier or more data-rich. However, it is necessary to establish the criteria that make an auxiliary task beneficial for a main task. Second, quantum data may carry different weights of importance in the optimization process. Focusing on the partial loss function of difficult data could lead to poorer generalization. We propose two principal approaches for these scenarios: task-based Q-CurL [Fig.1(a)], which determines the cur-

(a) Task-based Quantum Curriculum Learning



(b) Data-based Quantum Curriculum Learning

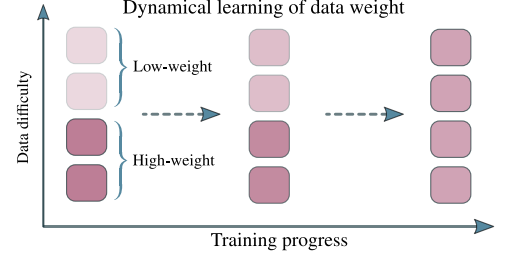


FIG. 1. Overview of two principal methodologies in quantum curriculum learning: (a) task-based and (b) data-based approaches. In the task-based approach, a model \mathcal{M} , designated for a main task that may be challenging or constrained by data accessibility, benefits from pre-training on an auxiliary task. This auxiliary task is either relatively simpler (left panel of (a)) or has a richer dataset (right panel of (a)). In the data-based approach, we implement a dynamic learning schedule to modulate data weights, thereby emphasizing the significance of quantum data in optimizing the loss function to reduce the generalization error.

riculum order based on the data density ratio between tasks, and data-based Q-CurL [Fig.1(b)], which employs a dynamic learning schedule that adjusts data weights, thereby prioritizing the importance of quantum data in the optimization. Empirical evidence demonstrates the utility of Q-CurL in enhancing training convergence and generalization when learning unitary dynamics. Furthermore, we show that data-based Q-CurL contributes to increased robustness in learning. Specifically, in scenarios with noisy labels, it can prevent complete memorization of the training data, thereby avoiding overfitting and enhancing generalization performance.

Task-based Q-CurL. — We formulate a framework for task-based Q-CurL. The target of learning is to find a function (or hypothesis, prediction model) $h : \mathcal{X} \rightarrow \mathcal{Y}$ within a hypothesis set \mathcal{H} that approximates the true function f mapping $\mathbf{x} \in \mathcal{X}$ to $\mathbf{y} = f(\mathbf{x}) \in \mathcal{Y}$ such that $h(\mathbf{x}) \approx f(\mathbf{x})$. To evaluate the correctness of the hypothesis h given the data (\mathbf{x}, \mathbf{y}) , the loss function $\ell : \mathcal{Y} \times \mathcal{Y} \rightarrow \mathbb{R}$ is used to measure the approximation error $\ell(h(\mathbf{x}), \mathbf{y})$ between the prediction $h(\mathbf{x})$ and the target \mathbf{y} . We aim to find a hypothesis $h \in \mathcal{H}$ that minimizes the expected risk over the distribution $P(\mathcal{X}, \mathcal{Y})$:

$$R(h) := \mathbb{E}_{(\mathbf{x}, \mathbf{y}) \sim P(\mathcal{X}, \mathcal{Y})} [\ell(h(\mathbf{x}), \mathbf{y})]. \quad (1)$$

In practice, since the data generation distribution $P(\mathcal{X}, \mathcal{Y})$ is unknown, we use the observed dataset $\mathcal{D} = (\mathbf{x}_i, \mathbf{y}_i)_{i=1}^N \subset \mathcal{X} \times \mathcal{Y}$ to minimize the empirical risk, defined as the average loss over the training data:

$$\hat{R}(h) = \frac{1}{N} \sum_{i=1}^N \ell(h(\mathbf{x}_i), \mathbf{y}_i). \quad (2)$$

Given a main task \mathcal{T}_M , the goal of task-based Q-CurL is to design a curriculum for solving auxiliary tasks to enhance performance compared to solving the main task alone. We consider $\mathcal{T}_1, \dots, \mathcal{T}_{M-1}$ as the set of auxiliary tasks. The training dataset for task \mathcal{T}_m is $\mathcal{D}_m \subset \mathcal{X}^{(m)} \times \mathcal{Y}^{(m)}$ ($m = 1, \dots, M$), containing N_m data

pairs. We focus on supervised learning tasks with input quantum data $\mathbf{x}_i^{(m)}$ in the input space $\mathcal{X}^{(m)}$ and corresponding target quantum data $\mathbf{y}_i^{(m)}$ in the output space $\mathcal{Y}^{(m)}$ for $i = 1, \dots, N_m$. The training data $(\mathbf{x}_i^{(m)}, \mathbf{y}_i^{(m)})$ for task \mathcal{T}_m are drawn from the probability distribution $P^{(m)}(\mathcal{X}^{(m)}, \mathcal{Y}^{(m)})$ with the density $p^{(m)}(\mathcal{X}^{(m)}, \mathcal{Y}^{(m)})$. We assume that all tasks share the same data spaces $\mathcal{X}^{(m)} \equiv \mathcal{X}$ and $\mathcal{Y}^{(m)} \equiv \mathcal{Y}$, as well as the same hypothesis h and loss function ℓ for all m .

Depending on the problem, we can decide the curriculum weight $c_{M,m}$, where a larger $c_{M,m}$ indicates a greater benefit of solving \mathcal{T}_m for improving the performance on \mathcal{T}_M . We evaluate the contribution of solving task \mathcal{T}_i to the main task \mathcal{T}_M by transforming the expected risk of training \mathcal{T}_M as follows:

$$\begin{aligned} R_{T_M}(h) &= \mathbb{E}_{(\mathbf{x}, \mathbf{y}) \sim P^{(M)}} [\ell(h(\mathbf{x}), \mathbf{y})] \\ &= \mathbb{E}_{(\mathbf{x}, \mathbf{y}) \sim P^{(m)}} \left[\frac{p^{(M)}(\mathbf{x}, \mathbf{y})}{p^{(m)}(\mathbf{x}, \mathbf{y})} \ell(h(\mathbf{x}), \mathbf{y}) \right]. \end{aligned} \quad (3)$$

The curriculum weight $c_{M,m}$ can be determined using the density ratio $r(\mathbf{x}, \mathbf{y}) = \frac{p^{(M)}(\mathbf{x}, \mathbf{y})}{p^{(m)}(\mathbf{x}, \mathbf{y})}$ without requiring the density estimation of $p^{(M)}(\mathbf{x}, \mathbf{y})$ and $p^{(m)}(\mathbf{x}, \mathbf{y})$. The key idea is to model $r(\mathbf{x}, \mathbf{y})$ using a linear model $\hat{r}(\mathbf{x}, \mathbf{y}) := \boldsymbol{\alpha}^\top \boldsymbol{\phi}(\mathbf{x}, \mathbf{y}) = \sum_{i=1}^{N_M} \alpha_i \phi_i(\mathbf{x}, \mathbf{y})$, where the vector of basis functions is $\boldsymbol{\phi}(\mathbf{x}, \mathbf{y}) = (\phi_1(\mathbf{x}, \mathbf{y}), \dots, \phi_{N_M}(\mathbf{x}, \mathbf{y}))$, and the parameter vector $\boldsymbol{\alpha} = (\alpha_1, \dots, \alpha_{N_M})^\top$ is learned from data [23].

The key factor that differentiates this framework from classical curriculum learning is the consideration of quantum data for \mathbf{x} and \mathbf{y} , which are assumed to be in the form of density matrices representing quantum states. Therefore, the basis function $\phi_l(\mathbf{x}, \mathbf{y})$ is naturally defined as the product of global fidelity quantum kernels used to compare two pairs of input and output quantum states as $\phi_l(\mathbf{x}, \mathbf{y}) = \text{Tr}[\mathbf{x}\mathbf{x}_l^{(M)}] \text{Tr}[\mathbf{y}\mathbf{y}_l^{(M)}]$. In this way, $R_{T_M}(h)$

can be approximated as:

$$R_{T_M}(h) \approx \frac{1}{N_M} \sum_{i=1}^{N_M} \hat{r}_\alpha(\mathbf{x}_i^{(m)}, \mathbf{y}_i^{(m)}) \ell(h(\mathbf{x}_i^{(m)}), \mathbf{y}_i^{(m)}). \quad (4)$$

The parameter vector α is estimated via the problem of minimizing $\frac{1}{2} \alpha^\top \mathbf{H} \alpha - \mathbf{h}^\top \alpha + \frac{\lambda}{2} \alpha^\top \alpha$, where we consider the regularization coefficient λ for L_2 -norm of α . Here, \mathbf{H} is the $N_M \times N_M$ matrix with elements $H_{l'l''} = \frac{1}{N_M} \sum_{i=1}^{N_M} \phi_l(\mathbf{x}_i^{(m)}, \mathbf{y}_i^{(m)}) \phi_{l''}(\mathbf{x}_i^{(m)}, \mathbf{y}_i^{(m)})$, and \mathbf{h} is the N_M -dimensional vector with elements $h_l = \frac{1}{N_M} \sum_{i=1}^{N_M} \phi_l(\mathbf{x}_i^{(m)}, \mathbf{y}_i^{(m)})$.

We consider each $\hat{r}_\alpha(\mathbf{x}_i^{(m)}, \mathbf{y}_i^{(m)})$ as the contribution of the data $(\mathbf{x}_i^{(m)}, \mathbf{y}_i^{(m)})$ from the auxiliary task \mathcal{T}_m to the main task \mathcal{T}_M . We define the curriculum weight $c_{M,m}$ as (see [23] for more details):

$$c_{M,m} = \frac{1}{N_M} \sum_{i=1}^{N_M} \hat{r}_\alpha(\mathbf{x}_i^{(m)}, \mathbf{y}_i^{(m)}). \quad (5)$$

We consider the unitary learning task to demonstrate the curriculum criteria based on $c_{M,m}$. We aim to optimize the parameters θ of a Q -qubit parameterized quantum circuit $U(\theta)$, such that, for the optimized parameters θ_{opt} , $U(\theta_{\text{opt}})$ can approximate an unknown Q -qubit unitary V ($U, V \in \mathcal{U}(\mathbb{C}^{2^Q})$).

Our goal is to minimize the Hilbert-Schmidt (HS) distance between $U(\theta)$ and V , defined as $C_{\text{HST}}(\theta) := 1 - \frac{1}{d^2} |\text{Tr}[V^\dagger U(\theta)]|^2$, where $d = 2^Q$ is the dimension of the Hilbert space. In the QML-based approach, we can access a training data set consisting of input-output pairs of pure Q -qubit states $\mathcal{D}_{\mathcal{Q}}(N) = \{(|\psi\rangle_j, V|\psi\rangle_j)\}_{j=1}^N$ drawn from the distribution \mathcal{Q} . If we take \mathcal{Q} as the Haar distribution, we can instead train using the empirical loss:

$$C_{\mathcal{D}_{\mathcal{Q}}(N)}(\theta) := 1 - \frac{1}{N} \sum_{j=1}^N |\langle \psi_j | V^\dagger U(\theta) | \psi_j \rangle|^2. \quad (6)$$

The parameterized ansatz unitary $U(\theta)$ can be modeled as $U(\theta) = \prod_{l=1}^L U^{(l)}(\theta_l)$, consisting of L repeating layers of unitaries. Each layer $U^{(l)}(\theta_l) = \prod_{k=1}^K \exp(-i\theta_{lk} H_k)$ is composed of K unitaries, where H_k are Hermitian operators, θ_l is a K -dimensional vector, and $\theta = \{\theta_1, \dots, \theta_L\}$ is the LK -dimensional parameter vector.

We present a benchmark of Q-CurL for learning the approximation of the unitary dynamics of the spin-1/2 XY model with the Hamiltonian $H_{XY} = \sum_{j=1}^Q (\sigma_j^x \sigma_{j+1}^x + \sigma_j^y \sigma_{j+1}^y + h_j \sigma_j^z)$, where $h_j \in \mathbb{R}$ and $\sigma_j^x, \sigma_j^y, \sigma_j^z$ are the Pauli operators acting on qubit j . This model is important in the study of quantum many-body physics, as it provides insights into quantum phase transitions and the behavior of correlated quantum systems.

To create the main task \mathcal{T}_M and auxiliary tasks, we represent the time evolution of H_{XY} via the ansatz V_{XY} , which is similar to the Trotterized version of $\exp(-i\tau H_{XY})$ [12]. The target unitary for the main task, $V_{XY}^{(M)} = \prod_{l=1}^{L_M} V^{(l)}(\beta_l) \prod_{l=1}^{L_F} V_{\text{fixed}}^{(l)}$, consists of $L_M = 20$ repeating layers, where each layer $V^{(l)}(\beta_l)$ includes parameterized z-rotations RZ (with assigned parameter β_l) and non-parameterized nearest-neighbor \sqrt{i} SWAP = $\exp(\frac{i\pi}{8}(\sigma_j^x \sigma_{j+1}^x + \sigma_j^y \sigma_{j+1}^y))$ gates. Additionally, we include the fixed-depth unitary $\prod_{l=1}^{L_F} V_{\text{fixed}}^{(l)}$ with $L_F = 20$ layers at the end of the circuit $V^{(l)}$ to increase expressivity. Similarity, keeping the same β_l , we create the target unitary for the auxiliary tasks \mathcal{T}_m as $V_{XY}^{(m)} = \prod_{l=1}^{L_m} V^{(l)}(\beta_l) \prod_{l=1}^{L_F} V_{\text{fixed}}^{(l)}$, with $L_m = 1, 2, \dots, 19$.

Figure 2(a) depicts the average HS distance over 100 trials of β_l and $V_{\text{fixed}}^{(l)}$ between the target unitary of each auxiliary task \mathcal{T}_m (with L_m layers) and the main task \mathcal{T}_M . We also plot the curriculum weight $c_{M,m}$ in Fig. 2(a) calculated in Eq. (5). Here, we consider the unitary V_{XY} learning with $Q = 4$ qubits via the hardware efficient ansatz $U_{\text{HEA}}(\theta)$ [23, 24] and use $N = 20$ Haar random states for input data $\mathbf{x}_i^{(m)}$ in each task \mathcal{T}_m . As depicted in Fig. 2(a), $c_{M,m}$ can capture the similarity between two tasks, as higher weights imply smaller HS distances.

Next, we propose a Q-CurL game to further examine the effect of Q-CurL. In this game, Alice has an ML model $\mathcal{M}(\theta)$ to solve the main task \mathcal{T}_M , but she needs to solve all the auxiliary tasks $\mathcal{T}_1, \dots, \mathcal{T}_{M-1}$ first. We assume the data forgetting in task transfer, meaning that after solving task A , only the trained parameters θ_A are transferred as the initial parameters for task B . We propose the following greedy algorithm to decide the curriculum order $\mathcal{T}_{i_1} \rightarrow \mathcal{T}_{i_2} \rightarrow \dots \rightarrow \mathcal{T}_{i_M=M}$ before training. Starting \mathcal{T}_{i_M} , we find the auxiliary task $\mathcal{T}_{i_{M-1}}$ ($i_{M-1} \in \{1, 2, \dots, M-1\}$) with the highest curriculum weights $c_{i_M, i_{M-1}}$. Similarity, to solve $\mathcal{T}_{i_{M-1}}$, we find the corresponding auxiliary task $\mathcal{T}_{i_{M-2}}$ in the remaining tasks with the highest $c_{i_{M-1}, i_{M-2}}$, and so on. Here, curriculum weights $c_{i_k, i_{k-1}}$ are calculated similarly to Eq. (5).

Figure 2(b) depicts the training and test loss of the main task \mathcal{T}_M (see Eq. (6)) for different training epochs and numbers of training data over 100 trials of parameters' initialization. In each trial, N Haar random states are used for training, and 20 Haar random states are used for testing. With a sufficient amount of training data ($N = 20$), introducing Q-CurL can significantly improve the trainability (lower training loss) and generalization (lower test loss) when compared with random order in Q-CurL game. Even with a limited amount of training data ($N = 10$), when overfitting occurs, Q-CurL still performs better than the random order.

Data-based Q-CurL.— We present a form of data-based Q-CurL that dynamically predicts the easiness of each sample at each training epoch, such that easy samples are emphasized with large weights during the early

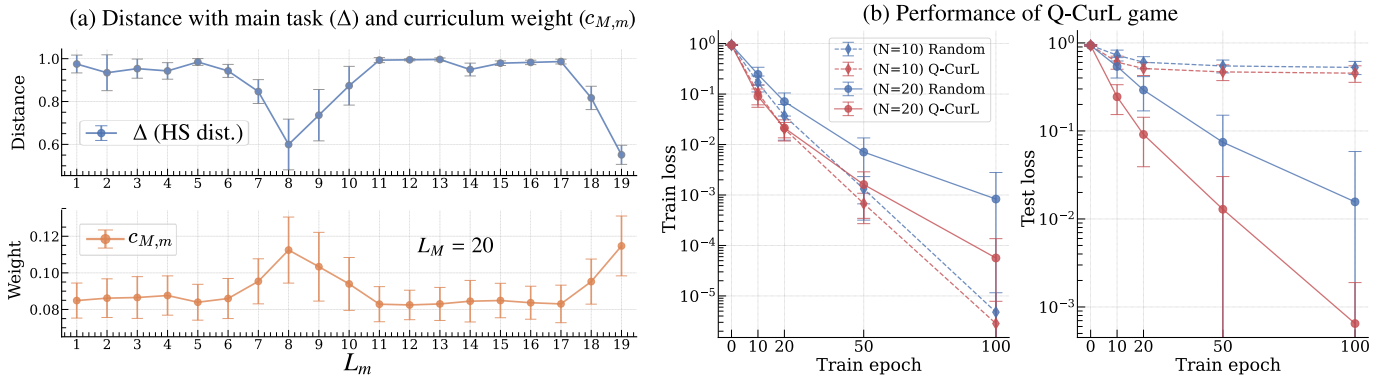


FIG. 2. (a) The curriculum weight (lower panel) and the Hilbert-Schmidt distance (upper panel) between the target unitary of the main task \mathcal{T}_M and the target unitary of the auxiliary task \mathcal{T}_m . (b) The training loss and test loss for different training epochs and different numbers N of training data in the Q-CurL game, considering both random and Q-CurL orders. The average and standard deviations are calculated over 100 trials.

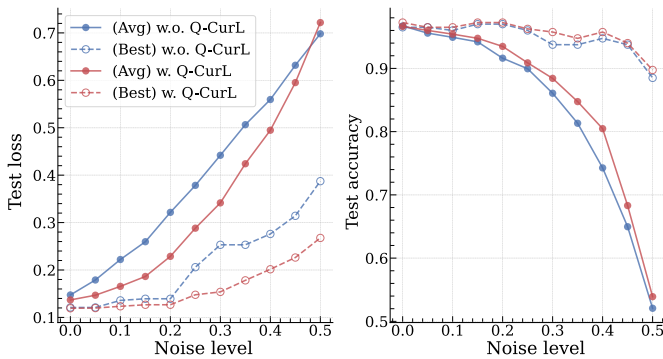


FIG. 3. The test loss and accuracy of the trained QCNN (with and without using the data-based Q-CurL) in the quantum phase recognition task with 8 qubits under varying noise levels in corrupted labels. Here, the average and the best performance over 50 trials are plotted.

stages of training and conversely. Apart from improving generalization, the benefit of data-based Q-CurL lies in its resistance to noise, which is especially needed in QML. Existing QML models can accurately fit partially corrupted labels to quantum states in the training data but fail on the test data [25]. We show that data-based Q-CurL can enhance the robustness based on the dynamic weighting of the difficulty fitting quantum data to corrupted labels.

Inspired by the confidence-aware techniques in classical ML [19–21], the idea is to modify the empirical risk as

$$\hat{R}(h, \mathbf{w}) = \frac{1}{N} \sum_{i=1}^N ((\ell_i - \eta)e^{w_i} + \gamma w_i^2). \quad (7)$$

Here, $\mathbf{w} = (w_1, \dots, w_N)$, $\ell_i = \ell(h(\mathbf{x}_i), \mathbf{y}_i)$, and w_i^2 is the regularization term controlled by the hyper-parameter $\gamma > 0$. The threshold η distinguishes easy and hard samples with e^{w_i} emphasizing the loss $\ell_i \ll \eta$ (easy sample) and neglecting the loss $\ell_i \gg \eta$ (hard samples, such as data

with corrupted labels). The minimization problem is reduced to $\min_{\theta} \min_{\mathbf{w}} \hat{R}(h, \mathbf{w})$, where θ is the parameter of the hypothesis h . Here, $\min_{\mathbf{w}} \hat{R}(h, \mathbf{w})$ is decomposed at each loss ℓ_i and solved without quantum resources as $w_i = \text{argmin}_{w_i} (\ell_i - \eta)e^{w_i} + \gamma w_i^2$. To control the difficulty of the samples, in each training epoch, we set η as the average value of all ℓ_i obtained from the previous epoch. Therefore, η changes dynamically during the early stages of training but remains almost constant during the convergence periods.

We apply the data-based Q-CurL to the quantum phase recognition task investigated in Ref. [10] to demonstrate that it can improve the generalization of the learning model. Here, we consider a one-dimensional cluster Ising model with open boundary conditions, whose Hamiltonian with Q qubits is given by $H = -\sum_{j=1}^{Q-2} \sigma_j^z \sigma_{j+1}^x \sigma_{j+2}^z - h_1 \sum_{j=1}^Q \sigma_j^x - h_2 \sum_{j=1}^{Q-1} \sigma_j^x \sigma_{j+1}^x$. Depending on the coupling constants (h_1, h_2), the ground state wave function of this Hamiltonian can exhibit multiple states of matter, such as the symmetry-protected topological phase, the paramagnetic state, and the anti-ferromagnetic state. We employ the quantum convolutional neural network (QCNN) model [10] with binary cross-entropy loss for training. Without Q-CurL, we use the conventional loss $\hat{R}(h) = (1/N) \sum_{i=1}^N \ell_i$ for the training and test phase. In data-based Q-CurL, we train the QCNN with the loss $\hat{R}(h, \mathbf{w})$ while using $\hat{R}(h)$ to evaluate the generalization on the test data set. We use 40 and 400 ground state wave functions for the training and test phase, respectively (see [23] for details of settings).

To evaluate the effectiveness of the data-based Q-CurL in considering the difficulty of the data in training, we consider the scenario of fitting corrupted labels. Given a probability p ($0 \leq p \leq 1$) representing the noise level, the true label $y_i \in \{0, 1\}$ of training state $|\psi_i\rangle$ is transformed to the label $1 - y_i$ with probability p , while it remains the true label with probability $1 - p$. Figure 3 illustrates the performance of trained QCNN on test data across

different noise levels. There is no significant difference at low noise levels, but as the noise level increases, the conventional training fails to generalize effectively. In this case, introducing data-based Q-CurL in training (red lines) reduces the test loss and enhances testing accuracy compared to the conventional method (blue lines).

Discussion.— The proposed Q-CurL framework can enhance training convergence and generalization in QML with quantum data. Future research should investigate whether Q-CurL can be designed to improve trainability in QML, particularly by avoiding the barren plateau problem. For instance, curriculum design is not limited to tasks and data but can also involve the progressive design of the loss function. Even when the loss function of the target task, designed for infeasibility in classical simulation to achieve quantum advantage [26, 27], is prone to the barren plateau problem, a well-designed sequence of classically simulable loss functions can be beneficial. Optimizing these functions in a well-structured curriculum before optimizing the main function may significantly improve the trainability and performance of the target task.

The authors acknowledge Koki Chinzei and Yuichi Kamata for their fruitful discussions. Special thanks are extended to Koki Chinzei for his valuable comments on the variations of the Q-CurL game, as detailed in the Supplementary Materials.

* tran.quochoan@fujitsu.com

- [1] J. Biamonte, P. Wittek, N. Pancotti, P. Rebentrost, N. Wiebe, and S. Lloyd, Quantum machine learning, *Nature* **549**, 195 (2017).
- [2] M. Schuld and F. Petruccione, *Machine Learning with Quantum Computers* (Springer International Publishing, 2021).
- [3] M. Schuld and N. Killoran, Is quantum advantage the right goal for quantum machine learning?, *PRX Quantum* **3**, 030101 (2022).
- [4] V. Havlíček, A. D. Córcoles, K. Temme, A. W. Harrow, A. Kandala, J. M. Chow, and J. M. Gambetta, Supervised learning with quantum-enhanced feature spaces, *Nature* **567**, 209 (2019).
- [5] M. Schuld and N. Killoran, Quantum machine learning in feature Hilbert spaces, *Phys. Rev. Lett.* **122**, 040504 (2019).
- [6] Y. Liu, S. Arunachalam, and K. Temme, A rigorous and robust quantum speed-up in supervised machine learning, *Nat. Phys.* (2021).
- [7] T. Goto, Q. H. Tran, and K. Nakajima, Universal approximation property of quantum machine learning models in quantum-enhanced feature spaces, *Phys. Rev. Lett.* **127**, 090506 (2021).
- [8] X. Gao, E. R. Anschuetz, S.-T. Wang, J. I. Cirac, and M. D. Lukin, Enhancing generative models via quantum correlations, *Phys. Rev. X* **12**, 021037 (2022).
- [9] Seeking a quantum advantage for machine learning, *Nat. Mach. Intell.* **5**, 813–813 (2023).
- [10] I. Cong, S. Choi, and M. D. Lukin, Quantum convolutional neural networks, *Nat. Phys.* **15**, 1273 (2019).
- [11] E. Perrier, A. Youssry, and C. Ferrie, Qdataset, quantum datasets for machine learning, *Sci. Data* **9**, 582 (2022).
- [12] T. Haug and M. S. Kim, Generalization with quantum geometry for learning unitaries, arXiv [10.48550/arXiv.2303.13462](https://arxiv.org/abs/10.48550/arXiv.2303.13462) (2023).
- [13] K. Chinzei, Q. H. Tran, K. Maruyama, H. Oshima, and S. Sato, Splitting and parallelizing of quantum convolutional neural networks for learning translationally symmetric data, *Phys. Rev. Res.* **6**, 023042 (2024).
- [14] Q. H. Tran, S. Kikuchi, and H. Oshima, Variational denoising for variational quantum eigensolver, *Phys. Rev. Res.* **6**, 023181 (2024).
- [15] L. Bittel and M. Kliesch, Training variational quantum algorithms is NP-hard, *Phys. Rev. Lett.* **127**, 120502 (2021).
- [16] E. R. Anschuetz and B. T. Kiani, Quantum variational algorithms are swamped with traps, *Nat. Commun.* **13**, 7760 (2022).
- [17] J. R. McClean, S. Boixo, V. N. Smelyanskiy, R. Babbush, and H. Neven, Barren plateaus in quantum neural network training landscapes, *Nat. Commun.* **9**, 4812 (2018).
- [18] Y. Bengio, J. Louradour, R. Collobert, and J. Weston, Curriculum learning, *Proceedings of the 26th Annual International Conference on Machine Learning ICML'09*, 41–48 (2009).
- [19] D. Novotny, S. Albanie, D. Larlus, and A. Vedaldi, Self-supervised learning of geometrically stable features through probabilistic introspection, in *2018 IEEE/CVF Conference on Computer Vision and Pattern Recognition* (IEEE, 2018).
- [20] S. Saxena, O. Tuzel, and D. DeCoste, Data parameters: A new family of parameters for learning a differentiable curriculum, in *Advances in Neural Information Processing Systems*, Vol. 32, edited by H. Wallach, H. Larochelle, A. Beygelzimer, F. d'Alché-Buc, E. Fox, and R. Garnett (Curran Associates, Inc., 2019).
- [21] T. Castells, P. Weinzaepfel, and J. Revaud, Super-loss: A generic loss for robust curriculum learning, in *Advances in Neural Information Processing Systems*, Vol. 33, edited by H. Larochelle, M. Ranzato, R. Hadsell, M. Balcan, and H. Lin (Curran Associates, Inc., 2020) pp. 4308–4319.
- [22] A. Mari, T. R. Bromley, J. Izaac, M. Schuld, and N. Killoran, Transfer learning in hybrid classical-quantum neural networks, *Quantum* **4**, 340 (2020).
- [23] See Supplemental Materials for details of the derivation of the curriculum weight in the task-based Q-CurL, the model and data's settings of quantum phase recognition task, the minimax framework in transfer learning, and several additional results, which include Refs. [28–31].
- [24] P. K. Barkoutsos, J. F. Gonthier, I. Sokolov, N. Moll, G. Salis, A. Fuhrer, M. Ganzhorn, D. J. Egger, M. Troyer, A. Mezzacapo, S. Filipp, and I. Tavernelli, Quantum algorithms for electronic structure calculations: Particle-hole hamiltonian and optimized wave-function expansions, *Phys. Rev. A* **98**, 022322 (2018).
- [25] E. Gil-Fuster, J. Eisert, and C. Bravo-Prieto, Understanding quantum machine learning also requires rethinking generalization, *Nat. Comm.* **15**, 2277 (2024).
- [26] M. Cerezo, M. Larocca, D. García-Martín, N. L. Diaz, P. Braccia, E. Fontana, M. S. Rudolph, P. Bermejo, A. Ijaz, S. Thanasilp, E. R. Anschuetz, and Z. Holmes, Does provable absence of barren plateaus imply classi-

- cal simulability? Or, why we need to rethink variational quantum computing, arXiv [10.48550/arxiv.2312.09121](https://arxiv.org/abs/10.48550/arxiv.2312.09121) (2023).
- [27] E. Gil-Fuster, C. Gyurik, A. Pérez-Salinas, and V. Dunjko, On the relation between trainability and dequantization of variational quantum learning models, arXiv [10.48550/arXiv.2406.07072](https://arxiv.org/abs/10.48550/arXiv.2406.07072) (2024).
- [28] T. Kanamori, S. Hido, and M. Sugiyama, A least-squares approach to direct importance estimation, *J. Mach. Learn. Res.* **10**, 1391 (2009).
- [29] M. Sugiyama, T. Suzuki, and T. Kanamori, *Density Ratio Estimation in Machine Learning* (Cambridge University Press, 2012).
- [30] M. Mousavi Kalan, Z. Fabian, S. Avestimehr, and M. Soltanolkotabi, Minimax lower bounds for transfer learning with linear and one-hidden layer neural networks, in *Advances in Neural Information Processing Systems*, Vol. 33, edited by H. Larochelle, M. Ranzato, R. Hadsell, M. Balcan, and H. Lin (Curran Associates, Inc., 2020) pp. 1959–1969.
- [31] Z. Xu and A. Tewari, On the statistical benefits of curriculum learning, in *Proceedings of the 39th International Conference on Machine Learning*, Proceedings of Machine Learning Research, Vol. 162, edited by K. Chaudhuri, S. Jegelka, L. Song, C. Szepesvari, G. Niu, and S. Sabato (PMLR, 2022) pp. 24663–24682.

Supplementary Material for “Quantum Curriculum Learning”

Quoc Hoan Tran,* Yasuhiro Endo, and Hirotaka Oshima

Quantum Laboratory, Fujitsu Research, Fujitsu Limited, Kawasaki, Kanagawa 211-8588, Japan

(Dated: July 12, 2024)

This supplementary material describes in detail the calculations, the experiments presented in the main text, and the additional figures. The equation, figure, and table numbers in this section are prefixed with S (e.g., Eq. (S1) or Fig. S1, Table S1), while numbers without the prefix (e.g., Eq. (1) or Fig. 1, Table 1) refer to items in the main text.

CONTENTS

I. Task-based Q-CurL	1
A. Derive the curriculum weight	1
B. Unitary learning task	3
C. Minimax framework for transfer learning in unitary learning task	4
D. Additional results and other variations of the Q-CurL game	6
II. Quantum phase recognition task with data-based Q-CurL	7
References	8

I. TASK-BASED Q-CURL

A. Derive the curriculum weight

We formulate a framework for task-based Q-CurL to derive the curriculum weight. In classical ML, it is well-known that learning from multiple tasks can lead to better and more efficient algorithms. This idea encompasses areas such as transfer learning, multitask learning, and meta-learning, all of which have significantly advanced deep learning. Unlike classical ML, which typically assumes a fixed amount of training data for all tasks, in quantum learning, the order of tasks and the allocation of training data to each task are even more critical. Properly scheduling tasks could reduce the resources required for training the main task, bringing QML closer to practical, real-world applications.

The target of learning is to find a function (or hypothesis, prediction model) $h : \mathcal{X} \rightarrow \mathcal{Y}$ within a hypothesis set \mathcal{H} that approximates the true function f mapping $\mathbf{x} \in \mathcal{X}$ to $\mathbf{y} \in \mathcal{Y}$ such that $h(\mathbf{x}) \approx f(\mathbf{x})$. To evaluate the correctness of the hypothesis h given the data (\mathbf{x}, \mathbf{y}) , the loss function $\ell : \mathcal{Y} \times \mathcal{Y} \rightarrow \mathbb{R}$ is used to measure the approximation error $\ell(h(\mathbf{x}), \mathbf{y})$ between the prediction $h(\mathbf{x})$ and the target \mathbf{y} . We aim to find a hypothesis $h \in \mathcal{H}$ that minimizes the expected risk over the distribution $P(\mathcal{X}, \mathcal{Y})$:

$$R(h) := \mathbb{E}_{(\mathbf{x}, \mathbf{y}) \sim P(\mathcal{X}, \mathcal{Y})} [\ell(h(\mathbf{x}), \mathbf{y})]. \quad (\text{S1})$$

In practice, since the data generation distribution $P(\mathcal{X}, \mathcal{Y})$ is unknown, we use the observed dataset $\mathcal{D} = (\mathbf{x}_i, \mathbf{y}_i)_{i=1}^N \subset \mathcal{X} \times \mathcal{Y}$ to minimize the empirical risk (training loss), defined as the average loss over the training data:

$$\hat{R}(h) = \frac{1}{N} \sum_{i=1}^N \ell(h(\mathbf{x}_i), \mathbf{y}_i). \quad (\text{S2})$$

In a similar way, we can use Eq. (S2) to define the test loss as the average loss over the test data.

Given a main task \mathcal{T}_M , the goal of task-based Q-CurL is to design a curriculum for solving auxiliary tasks to enhance performance compared to solving the main task alone. We consider $\mathcal{T}_1, \dots, \mathcal{T}_{M-1}$ as the set of auxiliary tasks. The training dataset for task \mathcal{T}_m is $\mathcal{D}_m \subset \mathcal{X}^{(m)} \times \mathcal{Y}^{(m)}$ ($m = 1, \dots, M$), containing N_m data pairs. We focus on

* tran.quochoan@fujitsu.com

supervised learning tasks with input quantum data $\mathbf{x}_i^{(m)}$ in the input space $\mathcal{X}^{(m)}$ and corresponding target quantum data $\mathbf{y}_i^{(m)}$ in the output space $\mathcal{Y}^{(m)}$ for $i = 1, \dots, N_m$. The training data $(\mathbf{x}_i^{(m)}, \mathbf{y}_i^{(m)})$ for task \mathcal{T}_m are drawn from the probability distribution $P^{(m)}(\mathcal{X}^{(m)}, \mathcal{Y}^{(m)})$ with the density $p^{(m)}(\mathcal{X}^{(m)}, \mathcal{Y}^{(m)})$. We assume that all tasks share the same data spaces $\mathcal{X}^{(m)} \equiv \mathcal{X}$ and $\mathcal{Y}^{(m)} \equiv \mathcal{Y}$, as well as the same hypothesis h and loss function ℓ for all m in this framework. Depending on the problem, we can decide the curriculum weight $c_{M,m}$, where a larger $c_{M,m}$ indicates a greater benefit of solving \mathcal{T}_m for improving the performance on \mathcal{T}_M . We evaluate the contribution of solving task \mathcal{T}_i to the main task \mathcal{T}_M by transforming the expected risk of training \mathcal{T}_M as follows:

$$R_{T_M}(h) = \mathbb{E}_{(\mathbf{x}, \mathbf{y}) \sim P^{(M)}} [\ell(h(\mathbf{x}), \mathbf{y})] \quad (\text{S3})$$

$$= \int \int_{(\mathbf{x}, \mathbf{y})} \ell(h(\mathbf{x}), \mathbf{y}) p^{(M)}(\mathbf{x}, \mathbf{y}) d(\mathbf{x}, \mathbf{y}) \quad (\text{S4})$$

$$= \int \int_{(\mathbf{x}, \mathbf{y})} \frac{p^{(M)}(\mathbf{x}, \mathbf{y})}{p^{(m)}(\mathbf{x}, \mathbf{y})} \ell(h(\mathbf{x}), \mathbf{y}) p^{(m)}(\mathbf{x}, \mathbf{y}) d(\mathbf{x}, \mathbf{y}) \quad (\text{S5})$$

$$= \mathbb{E}_{(\mathbf{x}, \mathbf{y}) \sim P^{(m)}} \left[\frac{p^{(M)}(\mathbf{x}, \mathbf{y})}{p^{(m)}(\mathbf{x}, \mathbf{y})} \ell(h(\mathbf{x}), \mathbf{y}) \right]. \quad (\text{S6})$$

The curriculum weight $c_{M,m}$ can be determined using the density ratio $r(\mathbf{x}, \mathbf{y}) = \frac{p^{(M)}(\mathbf{x}, \mathbf{y})}{p^{(m)}(\mathbf{x}, \mathbf{y})}$ without requiring the density estimation of $p^{(M)}(\mathbf{x}, \mathbf{y})$ and $p^{(m)}(\mathbf{x}, \mathbf{y})$. Similar to the unconstrained least-squares importance fitting approach [1] in classical ML, the key idea is to model the density ratio function $r(\mathbf{x}, \mathbf{y})$ using a linear model:

$$\hat{r}(\mathbf{x}, \mathbf{y}) := \boldsymbol{\alpha}^\top \boldsymbol{\phi}(\mathbf{x}, \mathbf{y}) = \sum_{i=1}^{N_M} \alpha_i \phi_i(\mathbf{x}, \mathbf{y}), \quad (\text{S7})$$

where the vector of basis functions is $\boldsymbol{\phi}(\mathbf{x}, \mathbf{y}) = (\phi_1(\mathbf{x}, \mathbf{y}), \dots, \phi_{N_M}(\mathbf{x}, \mathbf{y}))$, and the parameter vector $\boldsymbol{\alpha} = (\alpha_1, \dots, \alpha_{N_M})^\top$ is learned from data.

The key factor that differentiates this framework from classical curriculum learning is the consideration of quantum data for \mathbf{x} and \mathbf{y} , which are assumed to be in the form of density matrices representing quantum states. Therefore, the basis function $\phi_l(\mathbf{x}, \mathbf{y})$ is naturally defined as the product of global fidelity quantum kernels used to compare two pairs of input and output quantum states as:

$$\phi_l(\mathbf{x}, \mathbf{y}) = \text{Tr}[\mathbf{x}\mathbf{x}_l^{(M)}] \text{Tr}[\mathbf{y}\mathbf{y}_l^{(M)}]. \quad (\text{S8})$$

In this way, $R_{T_M}(h)$ can be approximated by

$$R_{T_M}(h) \approx \mathbb{E}_{(\mathbf{x}, \mathbf{y}) \sim P^{(m)}} [\hat{r}_\alpha(\mathbf{x}, \mathbf{y}) \ell(h(\mathbf{x}), \mathbf{y})], \quad (\text{S9})$$

or, as an approximation, using the following sample averages:

$$R_{T_M}(h) \approx \frac{1}{N_m} \sum_{i=1}^{N_m} \hat{r}_\alpha(\mathbf{x}_i^{(m)}, \mathbf{y}_i^{(m)}) \ell(h(\mathbf{x}_i^{(m)}), \mathbf{y}_i^{(m)}). \quad (\text{S10})$$

The parameter vector $\boldsymbol{\alpha}$ is estimated by minimizing the following error:

$$\frac{1}{2} \int \int [\hat{r}_\alpha(\mathbf{x}, \mathbf{y}) - r(\mathbf{x}, \mathbf{y})]^2 p^{(m)}(\mathbf{x}, \mathbf{y}) d\mathbf{x} d\mathbf{y} \quad (\text{S11})$$

$$= \frac{1}{2} \int \int \hat{r}_\alpha(\mathbf{x}, \mathbf{y})^2 p^{(m)}(\mathbf{x}, \mathbf{y}) d\mathbf{x} d\mathbf{y} - \int \hat{r}_\alpha(\mathbf{x}, \mathbf{y}) p^{(M)}(\mathbf{x}, \mathbf{y}) d\mathbf{x} d\mathbf{y} + C. \quad (\text{S12})$$

Given the training data, we can further reduce the minimization of Eq. (S12) to the problem of minimizing

$$\frac{1}{2N_m} \sum_{i=1}^{N_m} \hat{r}_\alpha^2(\mathbf{x}_i^{(m)}, \mathbf{y}_i^{(m)}) - \frac{1}{N_M} \sum_{i=1}^{N_M} \hat{r}_\alpha(\mathbf{x}_i^{(M)}, \mathbf{y}_i^{(M)}) + \frac{\lambda}{2} \|\boldsymbol{\alpha}\|_2^2, \quad (\text{S13})$$

where we consider the regularization coefficient λ for L_2 -norm of $\boldsymbol{\alpha}$. Equation (S13) can be further reduced to the following quadratic form:

$$\min_{\boldsymbol{\alpha}} \frac{1}{2} \boldsymbol{\alpha}^\top \mathbf{H} \boldsymbol{\alpha} - \mathbf{h}^\top \boldsymbol{\alpha} + \frac{\lambda}{2} \boldsymbol{\alpha}^\top \boldsymbol{\alpha}. \quad (\text{S14})$$

Here, \mathbf{H} is the $N_M \times N_M$ matrix with elements $H_{ll'} = \frac{1}{N_m} \sum_{i=1}^{N_m} \phi_l(\mathbf{x}_i^{(m)}, \mathbf{y}_i^{(m)}) \phi_{l'}(\mathbf{x}_i^{(m)}, \mathbf{y}_i^{(m)})$, and \mathbf{h} is the N_M -dimensional vector with elements $h_l = \frac{1}{N_m} \sum_{i=1}^{N_m} \phi_l(\mathbf{x}_i^{(m)}, \mathbf{y}_i^{(m)})$.

In the task-based Q-CurL framework, we can consider each $\hat{r}(\mathbf{x}_i^{(m)}, \mathbf{y}_i^{(m)})$ in Eq. (S10) as the contribution of the data $(\mathbf{x}_i^{(m)}, \mathbf{y}_i^{(m)})$ from the auxiliary task \mathcal{T}_m to the main task \mathcal{T}_M . From Eq. (S10), we note that only the quantity $\ell(h(\mathbf{x}_i^{(m)}), \mathbf{y}_i^{(m)})$ depends on the training performance of the auxiliary task \mathcal{T}_m . We assume that the loss $\ell(h(\mathbf{x}_i^{(m)}), \mathbf{y}_i^{(m)})$ is bounded by a quantity $\ell_{\max}^{(m)}$ for all $i = 1, \dots, N_m$. Then the empirical risk $R_{T_M}(h)$ can be bounded by the following inequality:

$$R_{T_M}(h) \approx \frac{1}{N_m} \sum_{i=1}^{N_m} \hat{r}_{\boldsymbol{\alpha}}(\mathbf{x}_i^{(m)}, \mathbf{y}_i^{(m)}) \ell(h(\mathbf{x}_i^{(m)}), \mathbf{y}_i^{(m)}) \leq \frac{\ell_{\max}^{(m)}}{N_m} \sum_{i=1}^{N_m} \hat{r}_{\boldsymbol{\alpha}}(\mathbf{x}_i^{(m)}, \mathbf{y}_i^{(m)}) = \ell_{\max}^{(m)} c_{M,m}, \quad (\text{S15})$$

where

$$c_{M,m} = \frac{1}{N_m} \sum_{i=1}^{N_m} \hat{r}_{\boldsymbol{\alpha}}(\mathbf{x}_i^{(m)}, \mathbf{y}_i^{(m)}). \quad (\text{S16})$$

Therefore, $c_{M,m}$ evaluates the effect of minimizing $\ell_{\max}^{(m)}$ (of the auxiliary task \mathcal{T}_m) on the empirical risk in training the main task \mathcal{T}_M . A large (small) $c_{M,m}$ means that reducing $\ell_{\max}^{(m)}$ has a greater (less) contribution to minimizing $R_{T_M}(h)$. In our task-based Q-CurL framework, we define $c_{M,m}$ as the curriculum weight.

B. Unitary learning task

As a demonstration of the curriculum criteria based on $c_{M,m}$, we consider the unitary learning task. Here, we aim to optimize the parameters $\boldsymbol{\theta}$ of a Q -qubit parameterized quantum circuit $U(\boldsymbol{\theta})$, such that, for the optimized parameters $\boldsymbol{\theta}_{\text{opt}}$, $U(\boldsymbol{\theta}_{\text{opt}})$ can approximate an unknown Q -qubit unitary V ($U, V \in \mathcal{U}(\mathbb{C}^{2^Q})$). Our goal is to minimize the Hilbert-Schmidt (HS) distance between $U(\boldsymbol{\theta})$ and V , defined as:

$$C_{\text{HST}}(\boldsymbol{\theta}) := 1 - \frac{1}{d^2} |\text{Tr}[V^\dagger U(\boldsymbol{\theta})]|^2, \quad (\text{S17})$$

where $d = 2^Q$ is the dimension of the Hilbert space. This HS distance is equivalent to the average fidelity between two evolved states under $U(\boldsymbol{\theta})$ and V from the same initial state $|\psi\rangle$ drawn from the Haar uniform distribution of states:

$$C_{\text{HST}}(\boldsymbol{\theta}) = \frac{d+1}{d} \mathbb{E}_{|\psi\rangle \sim \text{Haar}_n} [1 - |\langle \psi | V^\dagger U(\boldsymbol{\theta}) | \psi \rangle|^2]. \quad (\text{S18})$$

This suggests a QML-based approach to learn the target unitary V , where we can access a training data set consisting of input-output pairs of pure Q -qubit states $\mathcal{D}_{\mathcal{Q}}(N) = \{(|\psi\rangle_j, V|\psi\rangle_j)\}_{j=1}^N$ drawn from the distribution \mathcal{Q} . If we take \mathcal{Q} as the Haar distribution, we can instead train using the empirical loss

$$C_{\mathcal{D}_{\mathcal{Q}}(N)}(\boldsymbol{\theta}) := 1 - \frac{1}{N} \sum_{j=1}^N |\langle \psi_j | V^\dagger U(\boldsymbol{\theta}) | \psi_j \rangle|^2. \quad (\text{S19})$$

In variational quantum algorithms, the parameterized ansatz unitary $U(\boldsymbol{\theta})$ can be modeled as $U(\boldsymbol{\theta}) = \prod_{l=1}^L U^{(l)}(\boldsymbol{\theta}_l)$, consisting of L repeating layers of unitaries. Each layer $U^{(l)}(\boldsymbol{\theta}_l) = \prod_{k=1}^K \exp(-i\theta_{lk} H_k)$ is composed of K unitaries, where H_k are Hermitian operators, $\boldsymbol{\theta}_l$ is a K -dimensional vector, and $\boldsymbol{\theta} = \{\boldsymbol{\theta}_1, \dots, \boldsymbol{\theta}_L\}$ is the LK -dimensional parameter vector.

We present a benchmark of Q-CurL for learning the approximation of the unitary dynamics for the spin-1/2 XY model with the following Hamiltonian:

$$H_{XY} = \sum_{j=1}^Q (\sigma_j^x \sigma_{j+1}^x + \sigma_j^y \sigma_{j+1}^y + h_j \sigma_j^z), \quad (\text{S20})$$

where $h_j \in \mathbb{R}$ and $\sigma_j^x, \sigma_j^y, \sigma_j^z$ are the Pauli operators acting on qubit j . This model is important in the study of quantum many-body physics, as it provides insights into quantum phase transitions and the behavior of correlated quantum systems.

To create the situation of main task \mathcal{T}_M and auxiliary tasks, we represent the time evolution of H_{XY} via the ansatz V_{XY} , which is similar to the Trotterized version of $\exp(-i\tau H_{XY})$ [2]. The unitary for the main task consisting of $L_M = 20$ repeating layers is defined as follows:

$$V_{XY}^{(M)} = \prod_{l=1}^{L_M} V^{(l)}(\beta_l) \prod_{l=1}^{L_F} V_{\text{fixed}}^{(l)}, \quad (\text{S21})$$

where each layer $V^{(l)}(\beta_l)$ includes parameterized z-rotations RZ (with assigned parameter β_l) and non-parameterized nearest-neighbor $\sqrt{i\text{SWAP}} = \exp(\frac{i\pi}{8}(\sigma_j^x \sigma_{j+1}^x + \sigma_j^y \sigma_{j+1}^y))$ gates. Additionally, we include the fixed-depth unitary $\prod_{l=1}^{L_F} V_{\text{fixed}}^{(l)}$ with $L_F = 20$ layers at the end of the circuit $V^{(l)}$ to increase expressivity. Similarly, keeping the same parameters β_l , we create the target unitary for the auxiliary tasks \mathcal{T}_m as

$$V_{XY}^{(m)} = \prod_{l=1}^{L_m} V^{(l)}(\beta_l) \prod_{l=1}^{L_F} V_{\text{fixed}}^{(l)}, \quad (\text{S22})$$

with $L_m = 1, 2, \dots, 19$.

In our experiments, we consider the unitary $V_{XY}^{(m)}$ learning with $Q = 4$ qubits via the hardware efficient ansatz $U_{\text{HEA}}(\theta)$. This ansatz comprises multiple blocks, where each block consists of single-qubit operations spanned by SU(2) on all qubits and two-qubit controlled-X entangling gates [3] repeated for all pairs of neighbor qubits. Here, we use rotation operators of Pauli Y and Z as single qubit gates. Mathematically, $U_{\text{HEA}}(\theta)$ is defined as follows:

$$U_{\text{HEA}}(\theta) = \prod_{l=1}^{L_E} \left(\prod_{q=1}^Q [U_R^{q,l}(\theta)] \times U_{\text{Ent}} \right) \times \prod_{q=1}^Q [U_R^{q,0}(\theta)],$$

with Q qubits consisting of L_E entangling gates U_{Ent} alternating with $Q(L_E + 1)$ rotation gates on each qubit. Here, we use $U_R(\theta) = R_Y(\theta_1)R_Z(\theta_2)$, and U_{Ent} is composed of CNOT gates placed in linear with indexes $(q, q + 1)$ of qubits. The number of parameters in this circuit is $Q(2L_E + 1)$.

C. Minimax framework for transfer learning in unitary learning task

The task-based Q-CurL framework leaves several fundamental questions regarding the implementation of transfer learning algorithms from an auxiliary task to a main task. For example, what is the best accuracy that can be achieved through any transfer learning algorithm? How does this accuracy depend on the transferability between tasks? How does the accuracy of the main task in transfer learning scale with the amount of data in both the auxiliary and main tasks? In this section, we formulate the general minimax framework for transfer learning within the task-based Q-CurL framework. Specifically, for the unitary learning task, we map the minimax lower bounds for transfer learning with parameterized quantum circuits to the derivation of minimax lower bounds in transfer learning for linear regression problems. However, the detailed form of this bound is left for future research.

Here, we focus on the unitary learning task. We assume the presence of an auxiliary task \mathcal{T}_m and a main task \mathcal{T}_M , with target unitaries V_m and V_M ($V_m, V_M \in \mathcal{U}(\mathbb{C}^{2^Q})$), respectively. In the auxiliary task, we can access a training data set \mathcal{A}_m consisting of N_m input-output pairs of Q -qubits states as $\mathcal{A}_m = \left\{ \left(|\psi_j^{(m)}\rangle, \mathcal{E}(V_m |\psi_j^{(m)}\rangle, \epsilon_j^{(m)}) \right) \right\}_{j=1}^{N_m}$, where \mathcal{E} is a quantum noise channel applied to the pure state $V_m |\psi_j\rangle$ with noise variable $\epsilon_j^{(m)}$. Here, $\epsilon_j^{(m)} = 0$ implies that the identity operator \mathcal{E} is applied to the quantum state. We assume that the output of \mathcal{E} is represented in the form of a density matrix. Similarly, in the main task \mathcal{T}_M , we have access to a training dataset \mathcal{A}_M consisting of

N_M input-output pairs of Q -qubit states, denoted as $\mathcal{A}_M = \left\{ \left(|\psi_j^{(M)}\rangle, \mathcal{E}(V_M |\psi_j^{(M)}\rangle, \epsilon_j^{(M)}) \right) \right\}_{j=1}^{N_M}$. Furthermore, we assume that the input data $|\psi_j^{(m)}\rangle$ and $|\psi_j^{(M)}\rangle$ for both tasks are drawn from the same distribution \mathcal{Q} , and each noise variable ϵ_j is drawn from a normal distribution $\mathcal{N}(0, \sigma^2)$ with mean zero and variance σ^2 .

With the notion of the HS distance between two unitaries as $\text{HS}(U, V) = 1 - \frac{1}{d^2} |\text{Tr}[V^\dagger U(\boldsymbol{\theta})]|^2$ ($d = 2^Q$), we formally define the transfer class of pairs of unitaries as

$$\mathcal{P}_\Delta = \{(U, V) | U, V \in \mathcal{U}(\mathbb{C}^d); \text{HS}(U, V) \leq \Delta\}. \quad (\text{S23})$$

In a transfer learning problem, we are interested in using both auxiliary and main training data to find an estimate of the target unitary V_M for the main task with a small generalization error. In the minimax approach, V_M is chosen in an adversarial way, and the goal is to find and estimate U_M that achieves the smallest worst-case target generalization risk (over the distribution \mathcal{Q}):

$$\sup_{\text{transfer class}} \mathbb{E}_{\text{auxiliary and main samples}} [\mathbb{E}_{\mathcal{Q}} \text{loss}]. \quad (\text{S24})$$

Formally, given an input data $|\psi_j^{(M)}\rangle \sim \mathcal{Q}$, the loss induced by this data and the estimated $U_M(\boldsymbol{\theta}_M)$ is expressed as

$$\ell_j(\boldsymbol{\theta}_M) = 1.0 - \langle \psi_j^{(M)} | U_M^\dagger(\boldsymbol{\theta}_M) \mathcal{E}(V_M |\psi_j^{(M)}\rangle, \epsilon_j^{(M)}) U_M(\boldsymbol{\theta}_M) | \psi_j^{(M)} \rangle. \quad (\text{S25})$$

Then, minimizing Eq. (S24) can be written as the following transfer learning minimax risk:

$$\mathcal{R}_M(\mathcal{P}_\Delta) := \inf_{\boldsymbol{\theta}_M} \sup_{(V_m, V_M) \in \mathcal{P}_\Delta} \mathbb{E}_{\mathcal{A}_m} \mathbb{E}_{\mathcal{A}_M} [\mathbb{E}_{\mathcal{Q}} \ell_j(\boldsymbol{\theta}_M)]. \quad (\text{S26})$$

We would like to know a lower bound on the transfer learning minimax risk in Eq. (S26) to characterize the fundamental limits of transfer learning. We note that this problem is very similar to the minimax framework in linear regression problems [4]. Generally, any Q -qubit density matrix ρ has a unique representation as

$$\rho = \frac{1}{2^Q} \sum_{j_{Q-1}=0}^3 \cdots \sum_{j_0=0}^3 r_{j_{Q-1}, \dots, j_0} \sigma_{j_{Q-1}} \otimes \cdots \otimes \sigma_{j_0}, \quad (\text{S27})$$

where $\sigma_0 = I, \sigma_1 = X, \sigma_2 = Y$, and $\sigma_3 = Z$ are the Pauli matrices. Therefore, the vector $(r_{j_{Q-1}, \dots, j_0})_{j_{Q-1}=0, \dots, j_0=0}^{j_{Q-1}=3, \dots, j_0=3} \in \mathbb{R}^{4^Q}$ can be considered as the multiqubit Bloch vector associated with ρ . The condition $\text{Tr}[\rho] = 1$ implies that $r_{0, \dots, 0} = 1$. Therefore, we can represent ρ with the vector form as

$$|\rho\rangle\rangle = \frac{1}{2^Q} \begin{pmatrix} 1 \\ \mathbf{r} \end{pmatrix}. \quad (\text{S28})$$

We can verify that $|\mathbf{r}| \leq \sqrt{2^Q - 1}$ and the equality occurs if and only if $\rho = |\psi\rangle\langle\psi|$ with $|\psi\rangle$ is a pure Q -qubit state. The i th element of $\begin{pmatrix} 1 \\ \mathbf{r} \end{pmatrix}$ is $\text{Tr}[P_i \rho]$, where $P_i = \sigma_{j_{Q-1}} \otimes \cdots \otimes \sigma_{j_0}$ is the i th Pauli string.

In general, a quantum channel \mathcal{E} acting on a density matrix ρ can be written as applying a matrix operator \hat{E} to the vector form of ρ as

$$|\mathcal{E}(\rho)\rangle\rangle = \hat{E} |\rho\rangle\rangle. \quad (\text{S29})$$

Here, \hat{E} is the Pauli transfer matrix (PTM) representation of the quantum channel \mathcal{E} , which is represented as

$$\hat{E} = \begin{pmatrix} 1 & \mathbf{0}^\top \\ \mathbf{b} & W \end{pmatrix}, \quad (\text{S30})$$

where $\mathbf{0} = (0, 0, \dots, 0) \in \mathbb{R}^{4^Q - 1}$, $\mathbf{b} \in \mathbb{R}^{4^Q - 1}$ and $W \in \mathbb{R}^{(4^Q - 1) \times (4^Q - 1)}$. Note that, if \mathcal{E} is a unitary channel then $\mathbf{b} = \mathbf{0}$.

With this PTM representation of the quantum channel, Eq. (S29) can be rewritten as

$$\mathbf{r}' = \mathbf{b} + W\mathbf{r}, \quad (\text{S31})$$

where $|\mathcal{E}(\rho)\rangle\rangle = \frac{1}{2^Q} \begin{pmatrix} 1 \\ \mathbf{r}' \end{pmatrix}$.

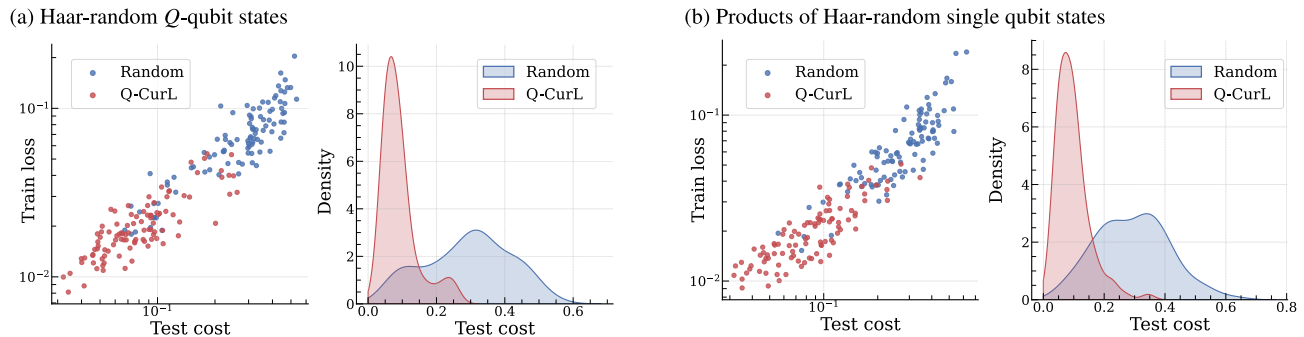


FIG. S1. The distribution and density of the training cost and test cost of the main task in the Q-CurL game, considering both random order and Q-CurL order based on the curriculum weights. Here, $N = 20$ random input data are trained for 20 epochs with 100 trials of initial parameters in the model, and $N = 20$ data are tested for each trained model. We consider two types of random input as (a) Haar-random Q -qubit states and (b) products of Q Haar-random single-qubit states.

We formulate the transfer learning minimax risk in terms of PTM representation. We define the matrix W in Eq. (S30) corresponding to unitary matrices V_m, V_M , and $U(\theta_M)$ as W_m, W_M , and $W(\theta_M)$, respectively. We also define the vector \mathbf{r} in Eq. (S28) corresponding to quantum states $|\psi_j^{(M)}\rangle$ as $\mathbf{r}_j^{(M)}$, and rewrite the PTM representation of the quantum channel $\mathcal{E}(\cdot, \epsilon_j^{(M)})$ as

$$\hat{\mathcal{E}}(\cdot, \epsilon_j^{(M)}) = \begin{pmatrix} 1 & \mathbf{0}^\top \\ \mathbf{b}(\epsilon_j^{(M)}) & W(\epsilon_j^{(M)}) \end{pmatrix}. \quad (\text{S32})$$

The loss function in Eq. (S25) can be expressed as

$$\ell_j(\theta_M) = \frac{1}{2^{Q+1}} \left\| W(\theta_M) \mathbf{r}_j^{(M)} - \left(W(\epsilon_j^{(M)}) W_M \mathbf{r}_j^{(M)} + \mathbf{b}(\epsilon_j^{(M)}) \right) \right\|^2 = \frac{1}{2^{Q+1}} \left\| \left(W(\theta_M) - W(\epsilon_j^{(M)}) W_M \right) \mathbf{r}_j^{(M)} - \mathbf{b}(\epsilon_j^{(M)}) \right\|^2 \quad (\text{S33})$$

Therefore, we can adapt the minimax framework to the linear regression setting, similar to approaches in the classical context [4]. It is essential to consider the requirements for \mathbf{r} to ensure it can represent a physical state and to specify the representations of the noise channel \mathcal{E} . For instance, if we only consider the unitary noise channel, then $\mathbf{b}(\epsilon_j^{(M)}) = \mathbf{0}$. We leave this intriguing aspect for future investigation.

D. Additional results and other variations of the Q-CurL game

Figure S1 depicts the distribution and density of the train loss and test loss of the main task in the Q-CurL game, comparing the Q-CurL order with a random order. Here, $N = 20$ random input data are trained for 20 epochs with 100 trials of initial parameters in the model, and $N = 20$ data are tested for each trained model. We consider two types of random inputs as (a) Haar-random Q -qubit states and (b) products of Q Haar-random single-qubit states. In both types of input states, the order in solving the Q-CurL game derived via the task-based Q-CurL method outperforms the performance when considering the random order.

The Q-CurL game setting and the heuristic greedy algorithm discussed in the main text demonstrate the usefulness of using curriculum weight to decide the curriculum order. We can further explore several variations of the Q-CurL game. For instance, instead of using the test loss $\mathcal{L}_t^{(M)}$ of the main task \mathcal{T}_M as the evaluation metric for the curriculum order $\mathcal{T}_{i_1} \rightarrow \mathcal{T}_{i_2} \rightarrow \dots \rightarrow \mathcal{T}_{i_M=M}$, one could consider minimizing the total test loss $\sum_{k=2}^M \mathcal{L}_t^{(i_k)}$. This approach would lead to a heuristic algorithm aimed at maximizing the total curriculum weights $\sum_{k=2}^M c_{i_k, i_{k-1}}$. Another variation is to consider the ‘‘task difficulty’’ perspective. For example, we could set the first task to be solved initially (as we know it is easy to solve, or we already have a trained model) and then determine an optimal task order that smoothly transitions from the first task to the main task.

II. QUANTUM PHASE RECOGNITION TASK WITH DATA-BASED Q-CURL

We apply the data-based Q-CurL to the quantum phase recognition task investigated in Ref. [5] to demonstrate that it can improve the generalization of the learning model. Here, we consider a one-dimensional cluster Ising model with open boundary conditions, whose Hamiltonian with Q qubits is given by

$$H = - \sum_{i=1}^{Q-2} \sigma_i^z \sigma_{i+1}^x \sigma_{i+2}^z - h_1 \sum_{i=1}^Q \sigma_i^x - h_2 \sum_{i=1}^{Q-1} \sigma_i^x \sigma_{i+1}^x. \quad (\text{S34})$$

Depending on the coupling constants (h_1, h_2) , the ground state wave function of this Hamiltonian can exhibit multiple states of matter, such as the symmetry-protected topological phase (SPT phase), the paramagnetic state, and the anti-ferromagnetic state.

We employ the quantum convolutional neural network (QCNN) model [5] to determine the matter phase of quantum states. Inspired by classical convolutional neural networks, the QCNN model consists of convolutional, pooling, and fully connected layers. The convolutional layers use local unitary gates to extract local features from the input data, while the pooling layers reduce the number of qubits. This alternation of layers ends in a fully connected layer that functions as a single convolution operator on the remaining qubits, providing an output through the measurement of the final qubit. The QCNN is governed by variational parameters that are optimized to classify training data accurately. In our implementation, the convolutional and fully connected layers are constructed using the Pauli decomposition of two-qubit unitary gates, expressed as $\prod_{j=1}^{15} e^{-i\theta_j P_j}$, where $\{P_j\}$ are the Pauli operators for two qubits, excluding the identity matrix. Each layer utilizes the same parameters for all unitary gates. Before measuring the output, we apply the Hadamard gate to the remaining qubit and then perform a measurement in the Z-basis.

For each training quantum data $|\psi_i\rangle$ and its corresponding label y_i , the QCNN produces the output q_i . The single loss ℓ_i is defined using the binary cross-entropy (BCE) loss as follows:

$$\ell_i = -y_i \log(\hat{y}_i) - (1.0 - y_i) \log(1.0 - \hat{y}_i), \quad (\text{S35})$$

where $\hat{y}_i = \text{sigmoid}(\mu q_i - 0.5)$. Here, we consider the scaling output with the coefficient $\mu = 2.0$. The label is predicted as 0 if $\hat{y}_i < 0.5$ and 1 if $\hat{y}_i \geq 0.5$. In the procedure without using the Q-CurL, we use the conventional loss $\hat{R}(h) = \frac{1}{N} \sum_{i=1}^N \ell_i$ for the training and testing phase. In data-based Q-CurL, we train the QCNN with the loss

$$\hat{R}(h, \mathbf{w}) = \frac{1}{N} \sum_{i=1}^N ((\ell_i - \eta)e^{w_i} + \gamma w_i^2), \quad (\text{S36})$$

and the procedure $\min_{\theta} \min_{\mathbf{w}} \hat{R}(h, \mathbf{w})$ mentioned in the main text. Here, $\min_{\mathbf{w}} \hat{R}(h, \mathbf{w})$ is decomposed at each loss ℓ_i and solved without quantum resources as

$$w_i = \text{argmin}_{\mathbf{w}} (l_i - \eta)e^{w_i} + \gamma w_i^2. \quad (\text{S37})$$

Since we consider the regularization parameter $\gamma > 0$, given $a = \frac{l_i - \eta}{\gamma}$, we can reduce Eq. (S37) into the following form: $w_i = \text{argmin}_{\mathbf{w}} g(w)$, with $g(w) = ae^w + w^2$ is the function of the scalar variable w . Here, we set $\gamma = 1.0$. To control the difficulty of the samples, in each training epoch, we set η as the average value of all ℓ_i obtained from the previous epoch. We use the conventional loss $\hat{R}(h)$ to evaluate the generalization on the test data set.

Similar to the setup in Ref. [5], we generate a training set of 40 ground state wave functions corresponding to $h_2 = 0$ and h_1 sampled at equal intervals in $[0.0, 1.6]$. The state is analytically solvable for these parameter choices, and this solution is used to label the training dataset (0 for the paramagnetic or antiferromagnetic phase and 1 for the SPT phase). The ground truth phase boundaries, which separate the two phases, are determined using DMRG simulations. Based on these boundaries, we also create a test dataset of 400 ground state wave functions corresponding to $h_2 \in \{0.8439, 0.6636, 0.5033, 0.3631, 0.2229, 0.09766, -0.02755, -0.1377, -0.2479, -0.3531\}$, and h_1 sampled 40 times at equal intervals in $[0.0, 1.6]$. The optimization is performed by the Adam method with a learning rate of 0.001 and 500 epochs of training.

In our experiment, we consider the scenario of fitting corrupted labels. Given a probability p ($0 \leq p \leq 1$) representing the noise level, the true label $y_i \in \{0, 1\}$ of quantum state $|\psi_i\rangle$ is transformed to the corrupted label $1 - y_i$ with probability p , while it remains the true label with probability $1 - p$.

Figure S2 illustrates the average performance of trained QCNN on test data with noise levels $p = 0.2, 0.3$ in corrupted training labels over different numbers of qubits. Introducing data-based Q-CurL (solid lines) in the training

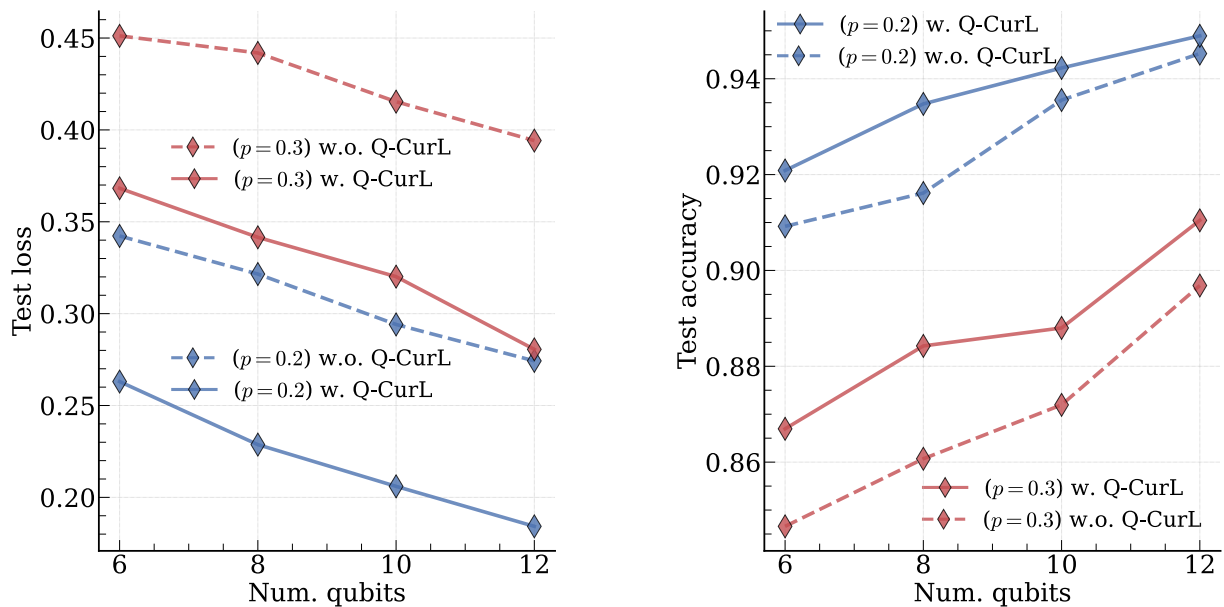


FIG. S2. The test loss (left panel) and test accuracy (right panel) of the trained QCNN on the quantum phase recognition task with (solid lines) or without (dotted lines) using the data-based Q-CurL over different numbers of qubits. Here, we consider two different noise levels in the corrupted training labels: $p = 0.2$ (blue) and $p = 0.3$ (red).

process reduces the test loss and enhances testing accuracy compared to the conventional training method (dotted lines). We note that introducing noise in the training labels leads to worse generalization in the system with fewer qubits. The small QCNN model struggles to extract the correct phase of the quantum data with limited information. However, as the number of qubits increases, more information is provided in the quantum wave functions for the QCNN to extract, thereby improving the robustness in phase detection tasks.

-
- [1] T. Kanamori, S. Hido, and M. Sugiyama, A least-squares approach to direct importance estimation, *J. Mach. Learn. Res.* **10**, 1391 (2009).
 - [2] T. Haug and M. S. Kim, Generalization with quantum geometry for learning unitaries, arXiv [10.48550/arXiv.2303.13462](https://arxiv.org/abs/10.48550/arXiv.2303.13462) (2023).
 - [3] P. K. Barkoutsos, J. F. Gonthier, I. Sokolov, N. Moll, G. Salis, A. Fuhrer, M. Ganzhorn, D. J. Egger, M. Troyer, A. Mezzacapo, S. Filipp, and I. Tavernelli, Quantum algorithms for electronic structure calculations: Particle-hole hamiltonian and optimized wave-function expansions, *Phys. Rev. A* **98**, 022322 (2018).
 - [4] M. Mousavi Kalan, Z. Fabian, S. Avestimehr, and M. Soltanolkotabi, Minimax lower bounds for transfer learning with linear and one-hidden layer neural networks, in *Advances in Neural Information Processing Systems*, Vol. 33, edited by H. Larochelle, M. Ranzato, R. Hadsell, M. Balcan, and H. Lin (Curran Associates, Inc., 2020) pp. 1959–1969.
 - [5] I. Cong, S. Choi, and M. D. Lukin, Quantum convolutional neural networks, *Nat. Phys.* **15**, 1273 (2019).